WISE: Warped Impulse Structure Estimation for Time-Domain Linear Macromodeling

Chi-Un Lei and Ngai Wong, *Member, IEEE*

***Abstract*— We develop a rational function macromodeling algorithm named warped impulse structure estimation for macromodeling of system responses with time-sampled data. The ideas of digital filter design, Walsh theorem, and complementary signal are introduced to convert the macromodeling problem into a non-pole-based Steiglitz–McBride iteration without initial guess and eigenvalue computation. Furthermore, we introduce frequency warping as a preprocessing step to improve the numerical condition in the computation. We demonstrate the fast convergence and the versatile macromodeling requirement adoption through a P-norm identification expansion, using examples from practical structures.**

***Index Terms*— Discrete-time domain, frequency warping, macromodeling, system identification, time domain.**

I. Introduction

With the increasing operation frequency and decreasing feature size of integrated circuits (ICs), high-frequency effects have become dominant factors that limit IC system performance. Therefore, in the design phase, accurate and efficient macromodeling is required to capture the high-frequency behaviors of systems for pre-layout simulation and signal integrity verification. However, a full-wave electromagnetic analysis over the global system is impractical. To generate reduced macromodels for efficient simulation, frequency-domain algorithms, such as vector fitting (VF) and its variants [1], have been used. Frequency-domain macromodeling requires spectral information which involves complicated measurement and capture of relatively long data sequences. Owing to its high computational cost, the full-wave analysis is usually terminated before all transient responses vanish so that truncated time responses are obtained. Macromodeling from truncated time-sampled data is therefore desirable.

In the past, subspace-based state-space system identification techniques [2] and generalized pencil-of-function methods [3] have been used for the identification of linear structures with time-sampled data. However, these methods are based on large-scale matrix operations and expensive singular value decomposition (SVD), and are less practical for macromodeling. VF-related techniques such as time-domain vector fitting (TD-VF) [4] and discrete-time domain vector fitting (TD-VFz) [5] have been developed for macromodeling of time-sampled data with lower computational cost, and they have also been extended to multiport/multiple-input-multiple-output (MIMO) macromodeling. However, their performance is limited by the numerically sensitive pole-basis calculation, expensive eigenvalue computation, and phase distortion due to nonlinear pole flipping.

In light of the discrete-time nature of the fixed time-step time-sampled response, a least-squares (LS) macromodeling technique (VISA) has been proposed recently [6], [7]. The idea is to regard the system response as a finite-length discrete response sequence of a finite-impulse-response (FIR) filter, and then an LS infinite-impulse-response (IIR) filter [8], usually of much lower order, is used to approximate the FIR response. This (low-order) IIR filter then provides a rational function capture of the macromodel. Compared to VF-based algorithms, VISA alleviates the computation in each iterative step and avoids the numerically sensitive eigenvalue computation, nonlinear pole flipping and initial pole assignment.

In this paper, we generalize VISA by introducing a frequency-warping process and propose warped impulse structure estimation (WISE) for efficient time-domain macromodeling. After the introduction in Section II, the mechanism of the core of WISE, the algorithm convergence analysis, convergence-related features (model order selection and P-norm identification) and MIMO extension are shown in Section III. Frequency warping, which redistributes the response spectral information for the ease of numerical computation, is proposed in Section IV. Macromodeling examples of real-world data in Section V then confirm the efficiency and accuracy of WISE.

II. Time-Domain Macromodeling

Multiport linear macromodeling aims at modeling a linear multiport structure with p input ports and q output ports, whose responses can be obtained by exciting one input port at a time and computing or measuring the responses at all output ports. A multiport macromodel is often cast as a MIMO transfer matrix with a common denominator (poles) and a specific numerator (zeros) for each port response, e.g., for the ease of generating SPICE circuit models. Macromodeling techniques intend to fit the rational function

$$\widehat{f}_{u,v}(s) = \frac{P_{u,v}(s)}{Q(s)} = \sum_{n=0}^{N} \frac{p_{u,v}(n)\, s^n}{q_n s^n} = d + \sum_{n=1}^{N} \frac{r_{u,v}(n)}{s - \alpha_n} \quad (1)$$

where $p_{u,v}(n), q(n) \in \mathbb{R}, q(0) = 1$, to the desired response $f_{u,v}(s)$ at a set of computed/measured points at input port

Manuscript received February 18, 2011; revised July 4, 2011; accepted July 24, 2011. Date of publication November 29, 2011; date of current version January 5, 2012. Recommended for publication by Associate Editor J. Tan upon evaluation of reviewers' comments.

The authors are with the Department of Electrical and Electronic Engineering, University of Hong Kong, Pokfulam, Hong Kong (e-mail: culei@eee.hku.hk; nwong@eee.hku.hk).

Color versions of one or more of the figures in this paper are available online at http://ieeexplore.ieee.org.

Digital Object Identifier 10.1109/TCPMT.2011.2170983

u ($1 \le u \le p$) and output port v ($1 \le v \le q$). The data points can be frequency-sampled data [i.e., $f_{u,v}(s_m)$, for $m = 1, 2, \ldots, N_s$] or discrete-time-sampled data (i.e., input response $W_{u,v}[m]$ and output response $Y_{u,v}[m]$, for $m = 0, 1, \ldots, L-1$). For ease of explanation, the single-input-single-output case is used in the following exposition. The extension to multiport macromodeling is presented in Section III-H.

In time-domain macromodeling, TD-VF [4], [9], a reformation of VF [1], attempts to fit the rational function (1) to a set of calculated/sampled data points at given time in the continuous-time domain with the help of a discretization process during each iteration. A discrete-time domain (i.e., z-domain) formulation of TD-VF, called TD-VFz, was proposed in [5]. TD-VFz is also a time-domain generalization from VFz [10], which is a z-domain formulation of VF. As in TD-VF, TD-VFz uses z-domain partial fractions to seek a rational approximation, $\widehat{F}(z)$, to the desired z-domain response $F(z)$ and exploits special features of z-domain macromodeling [11]. Furthermore, the convergence of TD-VFz is improved because of the omission of discretization process and the improved numerical condition for macromodeling. However, their performance is limited by the weak numerical properties of the iterative-based framework.

III. Core Formulation of WISE

Compared to existing algorithms, a promising observation in the core of WISE (the original VISA) is that, through a few generalizations, the identification problem boils down to finding an appropriate allpass operator. As a result, the numerator polynomial $P(z)$ and the denominator polynomial $Q(z)$ can be determined based on simple division algorithm, without exactly finding the location of poles. The exterior spectral processing part of WISE is discussed in Section IV.

In the following sections, the obtained output response is assumed to be generated by a normalized input pulse response [$w(0) = 1$ and $w(m) = 0$ for $m = 1, 2, \ldots, L-1$]. Therefore, we assume the input signal is a narrow Gaussian pulse signal, or the original output response is deconvoluted with the original input response. Then the output signal $y(t)$ is treated as a digital FIR filter response $H(z)$, and a digital IIR filter approximation algorithm [8] is applied to generate the linear macromodel.

A. Numerator Calculation

First, we define the error term $\Delta(z)$ as

$$\Delta(z) = H(z) - \left(\frac{P(z)}{Q(z)}\right) \tag{2}$$

where $H(z)$ is specified as an FIR filter response approximation of a system, and $H(z) = \sum_{m=0}^{L} h_m z^{-m}$, $h_m \in \mathbb{R}$ and $h_0 \neq 0$. Computing $P(z)/Q(z)$ requires nonlinear computations, but if poles $(\alpha_1, \alpha_2, \ldots, \alpha_N)$ are given, based on Walsh's theorem [12], the best L_2 approximation to $H(z)$ is the unique function that interpolates to $H(z)$ in all the points, where $z = \infty, 1/\alpha_1^*, 1/\alpha_2^*, \ldots, 1/\alpha_N^*$, and $*$ denotes complex conjugate. For the situation with no repeated poles, it means

$$H(z)|_{z=z_k} = \left.\frac{P(z)}{Q(z)}\right|_{z=z_k} \tag{3}$$

where $k = 0, 1, \ldots, N$, and (3) dictates that $\Delta(z)$ vanishes in the points z_k [12]. Since the approximant is the impulse response approximation of a system, the interpolation (3) is used to describe $\Delta(z)$, and can be represented by a cascade of a causal FIR filter $R(z)$ and an allpass filter $A(z)$ [13]

$$\Delta(z) = A(z)z^{-1}R(z) = \frac{z^{-N}Q(z^{-1})}{Q(z)}z^{-1}R(z) \tag{4}$$

where $R(z) = \sum_{m=0}^{L-1} r_m z^{-m}$ and the zeros of $A(z)$ are the interpolation points z_k. With (2), the interpolation problem can be expressed by

$$P(z) = H(z)Q(z) - z^{-(N+1)}Q\left(z^{-1}\right)R(z). \tag{5}$$

Through an elementwise vector flipping, (5) becomes

$$\begin{aligned} &Q(z)\left[z^{-(L-1)}R\left(z^{-1}\right)\right] \\ &= \left[z^{-L}H\left(z^{-1}\right)\right]\left[z^{-N}Q\left(z^{-1}\right)\right] - z^{-L}\left[z^{-N}P\left(z^{-1}\right)\right] \\ &\Rightarrow Y(z) = \frac{z^{-N}Q\left(z^{-1}\right)}{Q(z)}X_1(z) - \frac{z^{-L}}{Q(z)}X_2(z) \end{aligned} \tag{6}$$

where $U(z) = (z^{-L}H(z^{-1}))A(z) = \sum_{m=0}^{\infty} u_m z^{-m}$, $X_1(z) = z^{-L}H(z^{-1})$, $X_2(z) = z^{-N}P(z^{-1})$, and $Y(z) = z^{-(L-1)}R(z^{-1})$. An illustration of the digital filtering relationship in (6) is shown in Fig. 1. By equating the signal locations, (6) can be described as an input–output description of a digital filtering operation

$$r_{L-1-m} = u_m \quad (m = 0, 1, \ldots, L-1). \tag{7}$$

That is for the first L time instances, $[r_{L-1}r_{L-2}\cdots r_0] = [h_L h_{L-1}\cdots h_0] \otimes z^{-N}(Q(z^{-1})/Q(z))$ and $\otimes$ denotes the convolution.

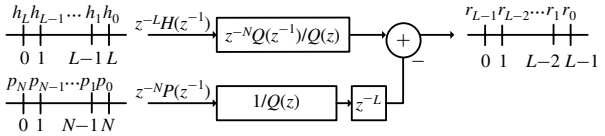

Fig. 1. Illustration of the digital filtering relationship in the interpolation problem (6).

B. Denominator Calculation

In numerical calculation, (4) is modified for designing an allpass operator $A^{(i)}(z)$ of a given order N, in the ith iteration, with

$$\begin{aligned} \Delta^{(i)}(z) &= A^{(i)}(z)z^{-1}R^{(i)}(z) \\ &= \frac{z^{-N}Q^{(i)}\left(z^{-1}\right)}{Q^{(i-1)}(z)}z^{-1}R^{(i)}(z). \end{aligned} \tag{8}$$

Since $\|\Delta^{(i)}(z)\| = \|R^{(i)}(z)\| = \|U^{(i)}(z)\|$ in (4) and (7), WISE involves a digital filtering operation (convolution) and

Algorithm 1 Pseudocodes of the core of WISE

1: Find $H(z)$, and $Q^{(0)}(z) := 1$;
2: **repeat**
3: Calculate $X^{(i)}(z)$ through (9) with the given $H(z)$ and $Q^{(i-1)}(z)$;
4: Construct $\mathbf{d}^{(i)}$ and $\mathbf{B}^{(i)}$ through elements of $X^{(i)}(z)$ by (11);
5: Calculate the new $Q_1^{(i)}(z)$ and $R^{(i)}(z)$ by (7) and (11);
6: **until** $Q_1^{(i)}(z)$ converges after N_T iterations;
7: Calculate $P(z)$ through (6) and (7) with the given $H(z)$, $Q^{(N_T)}(z)$ and $R^{(N_T)}(z)$;

a set of overdetermined equations to minimize $\|\Delta^{(i)}(z)\|$. First, we define $Q^{(0)}(z) := 1$, $Q^{(i)}(z) = 1 + Q_1^{(i)}(z)z^{-1}$, $Q_1^{(i)}(z) = \sum_{n=0}^{N-1} q^{(i)}(n+1)z^{-n}$, where $Q_1^{(i)}(z)$ contains transient characteristics of the system and is used in the interpolation. By (4), (7), and (8), a filtering operation (9) and a relationship (10) are set up to solve the LS problem (11)

$$X^{(i)}(z) = \sum_{n=0}^{\infty} x^{(i)}(n)\, z^{-n} = z^{-L}\frac{H\left(z^{-1}\right)}{Q^{(i-1)}(z)} \tag{9}$$

$$\begin{aligned} U^{(i)}(z) &= z^{-L}H\left(z^{-1}\right)\left(\frac{z^{-N}Q^{(i)}\left(z^{-1}\right)}{Q^{(i-1)}(z)}\right) \\ \Rightarrow U^{(i)}(z) &= X^{(i)}(z)z^{-N}\left(1+Q_1^{(i)}\left(z^{-1}\right)\right) \\ \Rightarrow U^{(i)}(z) &= z^{-N}X^{(i)}(z) + X^{(i)}(z)z^{-(N-1)}Q_1^{(i)}\left(z^{-1}\right) \end{aligned} \tag{10}$$

$$\min\left\|\Delta^{(i)}(z)\right\|_2 = \min\left\|U^{(i)}(z)\right\|_2 = \min\left\|\mathbf{B}^{(i)}\mathbf{q}^{(i)} - \mathbf{d}^{(i)}\right\|_2 \tag{11}$$

where $\mathbf{q}^{(i)} = [\, q^{(i)}(N) \cdots q^{(i)}(1)\,]^T$

$$\mathbf{d}^{(i)} = -\left[0 \;\cdots\; 0\; x^{(i)}(0) \;\cdots\; x^{(i)}(L-M-1)\right]^T$$

$$\mathbf{B}^{(i)} = \begin{bmatrix} x^{(i)}(0) & 0 & \cdots & 0 \\ x^{(i)}(1) & x^{(i)}(0) & \ddots & \vdots \\ \vdots & \vdots & \ddots & 0 \\ x^{(i)}(N-1) & x^{(i)}(N-2) & \cdots & x^{(i)}(0) \\ \vdots & \vdots & & \vdots \\ x^{(i)}(L-1) & x^{(i)}(L-2) & \cdots & x^{(i)}(L-N) \end{bmatrix}.$$

Allpass operator (8) converges after sufficient iterations N_T, and we take $Q(z) := Q^{(N_T)}(z)$. The pseudocodes summarizing the flow of the core of WISE is shown in Algorithm 1.

Some implementation remarks are in order.

1) $P(z)$ can be found analytically with the given polynomials $H(z)$, $Q(z)$, and $R(z)$ through (6) and (7), and $Q(z)$ can be obtained numerically from (7) and (11). Therefore, the macromodel can be obtained without knowing the location of poles [i.e., the zeros of $Q(z)$].
2) By applying Cauchy–Schwarz inequality, it is proved that for an arbitrary $X^{(i)}(z)$ which minimizes (11), the maximum pole (zeros of $Q(z)$) radius is always < 1, i.e., the macromodel is always stable [8]. Therefore, the macromodel phase response will not be deteriorated by the pole flipping technique used in VF.
3) WISE may not generate a passivity-guaranteed macromodel. However, passivity check/enforcement techniques in the continuous-time domain (as shown in [14]) can be used to rectify the model, since the bilinear continuous-to/from-discrete- transformation is passivity-preserving [15]. Furthermore, discussions about passivity in z-domain system can be found in [15].
4) WISE is proposed to identify fixed-time step responses. We may convert the variant time step response into fixed-time step response through downsampling and signal interpolations with considerations of sampling frequency [16]. However, the interpolated response may lose information in the densely sampled region due to the downsampling process.

C. WISE: Reformulation of Steiglitz–McBride (SM) Iteration

From (8), the objective function of WISE in the ith iteration becomes

$$\begin{aligned} &\min\sum_{j=0}^{L-1}\left|\Delta^{(i)}\left(z_j\right)\right|^2 = \min\sum_{j=0}^{L-1}\left|\frac{z^{-N}Q^{(i)}\left(z_j^{-1}\right)}{Q^{(i-1)}\left(z_j\right)}z^{-1}R^{(i)}\left(z_j\right)\right|^2 \\ &= \min\sum_{j=0}^{L-1}\frac{1}{\left|Q^{(i-1)}\left(z_j\right)\right|^2}\left|z^{-(N+1)}Q^{(i)}\left(z_j^{-1}\right)R^{(i)}\left(z_j\right)\right|^2 \\ &= \min\sum_{j=0}^{L-1}\frac{1}{\left|Q^{(i-1)}\left(z_j\right)\right|^2}\Big|Q^{(i)}\left(z_j\right)H\left(z_j\right) \\ &\qquad -\left(Q^{(i)}\left(z_j\right)H\left(z_j\right) - z^{-(N+1)}Q^{(i)}\left(z_j^{-1}\right)R^{(i)}\left(z_j\right)\right)\Big|^2 \\ &= \min\sum_{j=0}^{L-1}\frac{1}{\left|Q^{(i-1)}\left(z_j\right)\right|^2}\left|Q^{(i)}\left(z_j\right)H\left(z_j\right) - P^{(i)}\left(z_j\right)\right|^2. \end{aligned} \tag{12}$$

Consequently, WISE is considered as a reformulation of the SM iteration [17]. For sufficient order macromodels in white noise environments, the convergence rate of SM iteration is related to the signal-to-noise ratio (SNR) [18].

D. Macromodel Order Selection

As a reformulation of SM iteration, WISE provides *a priori* error bound for an Nth-order approximant, namely

$$\min_{\deg\left(\frac{P}{Q}\right)=N}\left(\frac{1}{2\pi}\int_{-\pi}^{\pi}\left|H(e^{j\omega}) - \frac{P^{(i)}(e^{j\omega})}{Q^{(i)}(e^{j\omega})}\right|^2 d\omega\right)^{\frac{1}{2}} \le \sigma_{N+1} \tag{13}$$

where σ_n stands for the nth Hankel singular values (HSVs). This error bound is important, as it provides a certificate for the identification accuracy and can be used to select the approximant order. It is shown that the singular value of an upper triangular Hankel matrix H is equivalent to the HSVs of the impulse response system [19]. The HSVs can be computed efficiently and arranged in descending magnitude

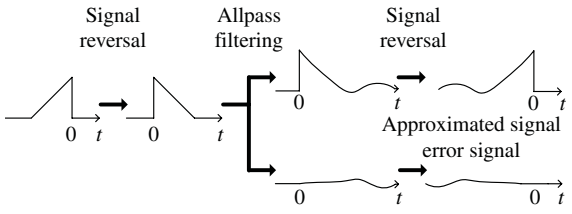

Fig. 2. Illustration about the complementary signal of a triangular signal.

characterizing the order of importance of each state. Exactly analogous to balanced truncation [19], the macromodel order N is chosen such that $\sigma_N \gg \sigma_{N+1}$. This approach gives a metric to determine an appropriate macromodel order.

E. Interpretation of the Algorithm Derivation Using Complementary Signal Concept

To calculate $Q(z)$, conventional methods have to extract response characteristics using eigenvalue calculations. WISE determines $Q(z)$ through an energy-conserved allpass filter characteristic, denoted as the *complementary signal* [20]. An illustration of the complementary signal of a triangular signal is shown in Fig. 2. First, the time-reversed response signal of the FIR filter $H(z)$ is defined as $\widetilde{H}[k]$, where $k = 0, 1, \ldots, L-1$. The idea of complementary signal is that, if $\widetilde{H}[k]$ is fed into the allpass filter $A(z)$ of which the time response is $A[m], m = 0, 1, \ldots$, then the energy of the allpass-filtered time-reversed signal $a[n] = A[m] \otimes \widetilde{H}[k]$ ($\otimes$ denotes convolution) is distributed as

$$\sum_{n=-\infty}^{\infty} |a[n]|^2 = \sum_{n=-L+1}^{\infty} |a[n]|^2 = \underbrace{\sum_{n=-L+1}^{0} |a[n]|^2}_{\Sigma_1} + \underbrace{\sum_{n=1}^{\infty} |a[n]|^2}_{\Sigma_2} \quad (14)$$

where Σ_1 is the approximation error energy and Σ_2 is the energy of the approximant. Through an allpass filtering and array operations, an arbitrary signal can be separated into an error signal and an approximant signal in the time domain. The algorithm objective is to design an N-th order allpass filter that minimizes the error energy, i.e., the energy within duration $0 \le n \le L-1$ during the energy redistribution [8], [20]. In WISE, an iterative approach is used to determine $A(z)$ by setting the energy minimization objective, which is described by (14), into the LS solving in (11).

F. Numerical Performance Comparison with Other Algorithms

As a simplification of SM iteration, WISE can be interpreted as a class of first-order interpolation and second-order interpolation problem [13]. Compared to the first-order interpolation (e.g., Padé approximation), SM iteration compensates the information of truncated responses (which always happens in time-domain macromodeling) during identification, generates stable macromodels and works robustly in noisy responses.

In the numerical sense, conventional SM iteration suffers from ill-conditioned calculation with hundreds of sampled data. Compared to other algorithms, WISE simplifies the numerical computation process, so it improves numerical accuracy and shortens computation time. WISE is also superior to other SM-related algorithms for the following reasons.

1) It uses frequency-/time-independent polynomial basis instead of frequency-/time-dependent pole-based basis. Therefore, it does not require initial-pole assignment (since $Q^{(0)}(z) := 1$), and its calculation is not deteriorated by: 1) the dynamic behavior and the initial guess of pole-based basis, and 2) the dynamic behavior of frequency/time parameters [21].
2) The denominator polynomial $Q(z)$ can be calculated through convolution (vector multiplication) and overdetermined equation-solving in (7) and (11). The numerator polynomial $P(z)$ can be numerically obtained through convolution and elementwise operation in (6) and (7), which does not involve any numerically sensitive calculations (e.g., root finding or numerical integration) and matrix operations. Therefore, the computation is numerically robust and efficient [22].

G. P-Norm Identification Criterion

The selection of identification criteria is important for system identification. The identified model should admit an exact description of the real system. An L_2-norm error prediction is usually used in VF. Other criterion extensions can also be developed for specific applications. The 2-norm (L_2) identification in (12) can be generalized to a P-norm (L_p) one, which meets different macromodeling requirements and gives a more realistic description of the system. For example, L_∞ (Chebyshev norm) identification gives a smaller macromodel for a linear-phase response, L_2 identification gives a more accurate macromodel for a noisy response, and L_1 identification is favorable for system identification with impulsive-noise-contaminated signals (outliers). For a P-norm identification, the minimization framework (12) is generalized to

$$\min \sum_{j=0}^{L-1} \left\| \Delta^{(i)}(z_j) \right\|_p = \min \left\| \mathbf{B}^{(i)} \mathbf{q}^{(i)} - \mathbf{d}^{(i)} \right\|_p = \min \sum_{j=0}^{L-1} \frac{1}{\left\| Q^{(i-1)}(z_j) \right\|_p} \left\| Q^{(i)}(z_j) H(z_j) - P^{(i)}(z_j) \right\|_p \quad (15)$$

for which the overdetermined equations (15) can be solved using any optimization tools (e.g., CVX [23]) effectively. It is noted that P-norm identification may deteriorate the L_2 convergence property, whereas L_∞-constrained L_2 identification can be used to guarantee the convergence.

H. Multiport System Macromodeling in WISE

VF-like algorithms require a large system equation to macromodel a multiport system, so the port splitting method is applied to fit a subset of port responses at one time, which are

then combined into a large macromodel [24]. Here, the transfer matrix with a common denominator is used so that Walsh's theorem can be applied to multiport macromodeling. The optimal numerator polynomial can be calculated through (6) and (7) by replacing $H(z)$ in (6) by $H_{u,v}(z)$. The common denominator is calculated by the same basis function for all port responses, then all the elements of $\mathbf{B_{p\times q}}$ are stacked into a single column of overdetermined equations

$$\begin{bmatrix} \mathbf{B}_{1,1}^{(i)} \\ \mathbf{B}_{1,2}^{(i)} \\ \vdots \\ \mathbf{B}_{p,q}^{(i)} \end{bmatrix} \left[\mathbf{q}^{(i)}\right] = \begin{bmatrix} \mathbf{d}_{1,1}^{(i)} \\ \mathbf{d}_{1,2}^{(i)} \\ \vdots \\ \mathbf{d}_{p,q}^{(i)} \end{bmatrix} \tag{16}$$

where $\mathbf{B}_{\mathbf{u,v}}^{(\mathbf{i})}$ and $\mathbf{d}_{u,v}^{(i)}$ are $\mathbf{B}$ and $\mathbf{d}$ in (11) for input port u ($1 \le u \le p$) and output port v ($1 \le v \le q$), respectively. The model order selection for the multiport macromodeling can be developed based on the derivation in Section III-D. A significant advantage of MIMO WISE is that it has an $O\left(N^2Lpq\right)$ complexity in each iteration in LS for the denominator polynomial calculation of a multiport system, whereas the original TD-VF and TD-VFz have an $O\left((pq+1)^2N^2Lpq\right)$ complexity for each iterative pole calculation, and other algorithms [2], [3] have an even higher computation complexity. Hence, significant memory storage and computation time can be saved by using WISE, which makes WISE a powerful macromodeling tool.

IV. Frequency Warping in WISE

In this section, the exterior z-domain spectral processing part of WISE is introduced. In short, the z-domain macromodeling is generalized to a frequency-warped z-domain ($\widetilde{z}$-domain) macromodeling for a better conditioned identification, through a parameter-controlled first-order mapping [25].

Frequency warping changes the signal sampling rate with respect to the frequency. It modifies the spectral distribution in order to achieve a better numerical condition. When the response is warped, the emphatic region of the frequency response is stretched and the remaining regions compressed, which gives a higher resolution (accuracy) in the emphatic frequency region and a lower resolution in other regions. The response is warped through a first-order allpass mapping, which preserves the model order and avoids numerical failure in long signal sequence transformation. Furthermore, frequency warping reduces the condition number, and thus delivers a more accurate solution. The warping also preserves the stability and optimality in the Chebyshev sense [26].

From a conformal mapping perspective, the warping starts by replacing the original variable z^{-1} by a new variable $\widetilde{z}^{-1}$. For example, distinct points z_1^{-1}, z_2^{-1}, and z_3^{-1} in the z-domain plane are mapped to distinct points $\widetilde{z}_1^{-1}$, $\widetilde{z}_2^{-1}$, and $\widetilde{z}_3^{-1}$ in the $\widetilde{z}$-domain plane. In our situation, z-domain dc is mapped to $\widetilde{z}$-domain dc (i.e., $z_1^{-1} = \widetilde{z}_1^{-1} = 1$) and half the sample rate in z-domain is mapped to half the sample rate in $\widetilde{z}$-domain (i.e., $z_2^{-1} = \widetilde{z}_2^{-1} = -1$) [25]. Therefore, the first-order (bilinear) transformation can be expressed by

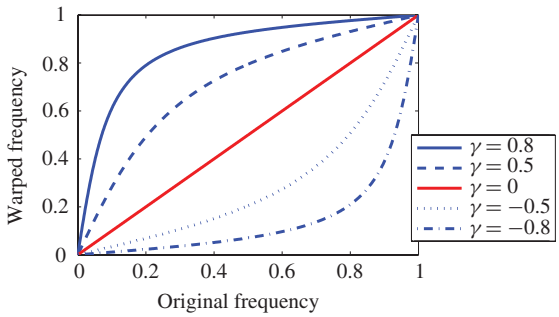

Fig. 3. Relationship of the sampled location between the z-domain (original frequency) and the $\widetilde{z}$-domain (warped frequency) with different warping parameters (γ).

$$\widetilde{z}^{-1} = \frac{z^{-1}+\gamma}{1+\gamma z^{-1}} \quad \text{and} \quad \gamma = \frac{\widetilde{z}_3^{-1} - z_3^{-1}}{1 - z_3^{-1}\widetilde{z}_3^{-1}} \tag{17}$$

where γ is the warping parameter to describe the emphatic location of the warped frequency response. The mapping of the sampled location between z-domain and $\widetilde{z}$-domain of some γ values is shown in Fig. 3. The mapping with $\gamma = 0$ gives the original mapping (i.e., $\widetilde{z} = z$). When $0 < \gamma < 1$, the warping gives a more accurate identification for the low-frequency region, rendering it suitable for practical macromodeling structures with lowpass responses.

From a z-domain system perspective, the warping starts by replacing the unit-delay operator z^{-1} in the original signal system $H(z)$ by an allpass operator $\widetilde{z}^{-1}$ in the system of the warped signal $G(\widetilde{z})$

$$H(z) \approx G(\widetilde{z}) \Leftrightarrow \sum_{m=0}^{L} h_m z^{-m} \approx \sum_{m=0}^{L} g_m \widetilde{z}^{-m}. \tag{18}$$

The warping of time-sampled response is performed through an allpass filtering, i.e., $g_m = \sum_{n=0}^{L} h_n \left(\widetilde{z}^{-1}(m)\right)^n$. After macromodeling in the $\widetilde{z}$ domain, the $\widetilde{z}$-domain approximant $\widehat{G}(\widetilde{z})$ can also be converted to the z-domain approximant $\widehat{H}(z)$ through an inverse bilinear transform of (17). Frequency warping can be applied for multiport macromodeling, by calculating the common poles of the macromodel in the warped domain and the numerator for each port response in the original domain.

The selection of the warping parameter γ is instrumental to an accurate identification. Although it is difficult to find the globally optimal γ due to its case dependence, we can select a γ that linearizes the frequency response in its corresponding domain, i.e., finding γ by $\min_{-1<\gamma<1} |(d^2/d\widetilde{z}^2)G(\widetilde{z})|$, as an empirical guess. γ can also be optimized using the bisection method with the identification error as the optimization criterion.

V. Numerical Examples

WISE is coded in MATLAB m-script files and run in the MATLAB 7.5 environment on a 1-GB RAM, 3.4-GHz PC. We use several practical examples to show the performance of WISE.

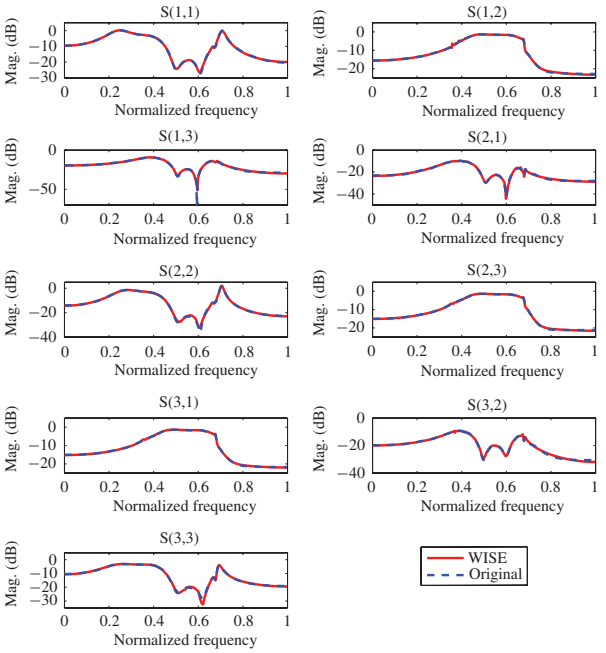

Fig. 4. Magnitude responses of S(u,v) of the circulator example using WISE in normalized frequency domain. S(u,v) is the scattering parameter at the input port u and output port v.

TABLE I
COMPARISON BETWEEN WISE AND TD-VF IN THE CIRCULATOR EXAMPLE

	25th order		32nd order	
	WISE	TD-VF	WISE	TD-VF
Max. deviation when converged	0.0019	0.0028	0.0011	0.0013
Avg. rms error when converged	0.0069	0.0085	0.0055	0.0051
CPU time for convergence (s)	4.07	64	5.72	77
CPU Time to −40-dB error (s)	3.10	38	4.29	44

A. Macrmodeling of a Three-Port RF Circulator

The first example is from a three-port counterclockwise RF circulator [27]. Time-domain transient scattering responses are computed ranging up to 4 GHz. All the nine port responses are excited and fitted simultaneously using the core WISE with a 25th-order macromodel. Time samples are taken at the intervals of 86 ps for the first 800 points (6.88 μs). The algorithm requires 13 iterations (4.07 s) to converge. Figs. 4 and 5 plot, respectively, the normalized frequency-domain responses and the time-domain responses of the converged approximant. Since there is a measurement defect at 0.68 f_s in the sampled data, WISE demonstrates robust and accurate fitting in both time and frequency domains. The model is also generated with TD-VF [9], which is commonly used in commercial tools (such as IdEM [24]). The quantitative comparison of both algorithms is shown in Table I. It shows that WISE is an accurate (18% less average rms error after convergence) and efficient algorithm ($>15\times$ faster for convergence and $>12\times$ faster to achieve a -40 dB accuracy). The data is further fitted using WISE and TD-VF with a 32nd-order macromodel. From Table I, WISE again generates a more accurate macromodel in the L_∞ sense and with more efficient computation. Fig. 6 shows the L_2 error during iterations for the two cases, showing that WISE converges much faster than TD-VF, due to the simple computation in WISE. In general, WISE converges quickly (within 60 iterations) for general responses, and actually faster for minimum-phase responses. We also check the robustness of the WISE by repeating the circulator example with a 25th-order model under an SNR of 30 dB. In this case, WISE converges with a -33.5 dB error.

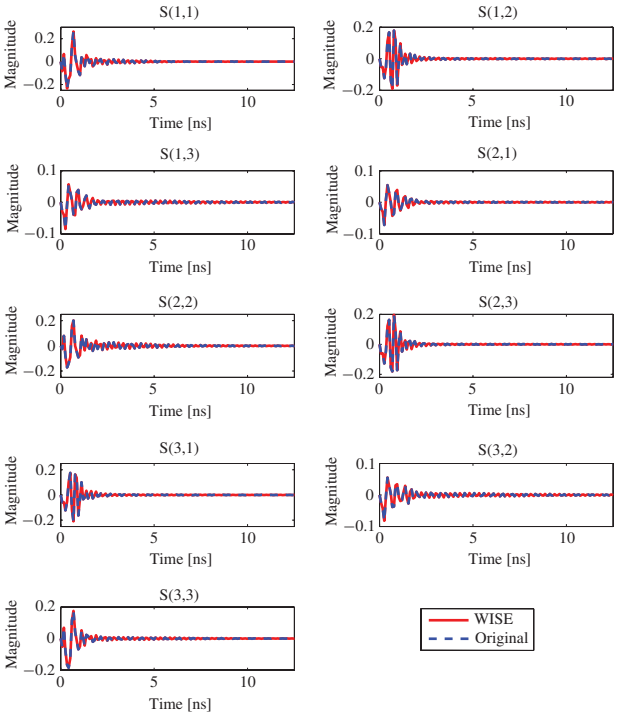

Fig. 5. Time responses of S(u,v) of the circulator example using WISE.

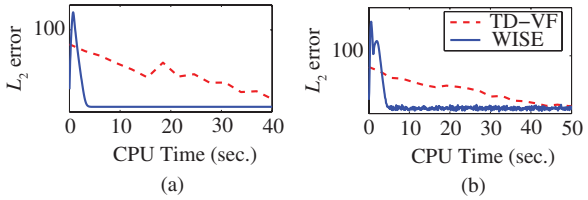

Fig. 6. L_2 error in macromodeling using TD-VF and WISE in the circulator example. (a) 25th-order macromodel. (b) 32nd-order macromodel.

B. Model Order Selection in WISE

Next, we investigate the use of HSVs in practical guiding the model order selection in WISE. Computing the HSVs of the example requires 3 s, and Fig. 7(a) shows the HSVs of the circulator example impulse responses. The figure shows a drop in HSVs, significant at first and gradual afterwards. Region of the largest HSVs and the relative error of different macromodel orders are shown in Fig. 7(b).

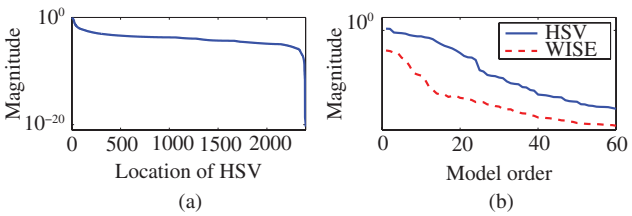

Fig. 7. HSVs of the system in the circulator example. (a) Entire HSVs. (b) Comparison with the macromodel error.

TABLE II
COMPARISON BETWEEN DIFFERENT P-NORM IDENTIFICATIONS, WHERE 2* REPRESENTS L_∞-CONSTRAINED 2-NORM IDENTIFICATION

P-norm approx.	L_1 err.	L_2 err.	L_∞ err.	CPU time (sec.)
1	0.0932	0.0111	0.0042	213.67
2 (CVX)	0.0674	0.0028	4.4e-4	4.44
∞	0.0664	0.0027	3.1e-4	7.05
2*	0.0657	0.0027	2.7e-4	3.35
2 (QR)	0.0674	0.0028	4.4e-4	0.11

C. P-Norm Identification in WISE

Response S(1, 1) has been extracted and fitted with the criteria of 1-norm, 2-norm, L_∞-constrained 2-norm, and ∞-norm, using CVX [23] and a 13th-order macromodel. The result is compared to the 2-norm criteria using QR decomposition (LSQR). The implementation details are shown in Table II. It shows that identifications can be faster (24.5 % CPU time reduction) and more accurate (3.5% L_2 error and 29.5% L_∞ error reduction) using nontraditional norm criteria, compared to LS-CVX identification. Compared to the original approach, P-norm identification can give a more accurate solution, at the expense of more computation time.

D. Macromodeling of a Time-Delayed Backplane Channel

This test example is from modeling an electrically long (40.5") differential transmission channel on a full mesh ATCA backplane [27]. The 750-point time-sampled response ranging up to 15 GHz is excited, normalized, and fitted using the core WISE. Since the delayed output signal cannot be fitted directly, the principal delay of the output signal is extracted by signal shifting before identification. The delay-extracted output signal is fitted with a 30-pole approximant, ending up at a relative error of -49.77 dB. It takes 5 iterations (0.0716 s) for WISE to reach convergence. The delay is included as $z^{-(T_d/T_s)}(P(z)/Q(z))$ during the post processing stage, where T_d is the delay time and T_s is the sampled time. Fig. 8(a) and (b) plot the fitting of the delay-extracted frequency-domain responses and the time-domain responses, respectively. Both show that WISE delivers excellent accuracy in modeling time-delayed responses, which often appear in on-board structures with high operating frequency.

E. Macromodeling of On-Chip Passive Structures

The four examples in [28] are from the macromodeling of measured two-port time responses of on-chip passive structures: a meander resistor (RPOLY2-ME), a spiral inductor (SP-SMALL), a coplanar line (U-COPL) and a metal-insulator-metal capacitor (CMIM). These on-chip passive structures often appear in compact and fully integrated chips. TD-VF cannot give a converged result for the first three examples, whereas the core WISE produces converged solutions for all cases. The quantitative comparison of the best result of TD-VF and the converged result of WISE is shown in Table III, generating macromodel with 51% less L_2 error on average and much faster computation.

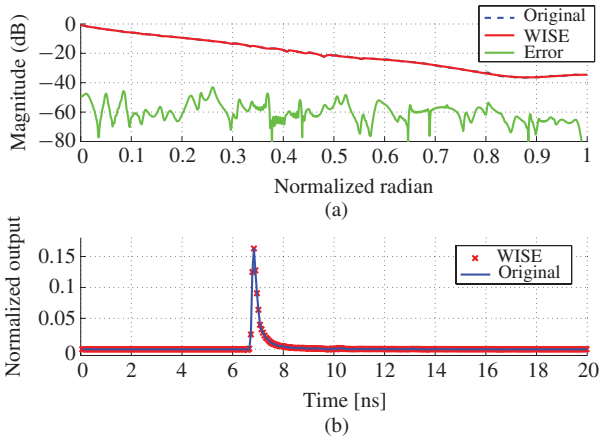

Fig. 8. Response of the differential channel example using WISE. (a) Magnitude response with delay extraction in normalized frequency domain. (b) Time domain response.

TABLE III
COMPARISON BETWEEN WISE AND TD-VF IN THE ON-CHIP STRUCTURE EXAMPLES. THE BRACKETED VALUE IS THE TD-VF RESULT

	Max. deviation	Avg. rms error	CPU (s)
RPOLY2-ME	0.0002(0.0004)	0.0006(0.0008)	0.24(8)
CMIM	0.0001(0.0032)	0.0005(0.0149)	0.40(8)
SP-SMALL	0.0003(0.0008)	0.0007(0.0027)	0.63(8)
U-COPL	0.0003(0.0004)	0.0010(0.0011)	0.21(7)

F. Frequency Warping in WISE

Examples of the backplane in Section V-D are used for demonstration. The 500-point time-sampled response of a differential channel in the backplane is sampled at 3-ps intervals. The response is delay-extracted and warped using (17) and identified with a 40-pole approximant, where γ is optimized using the bisection method. Fig. 9(a) plots the normalized frequency responses of the original signal (z-domain), the warped signal ($\tilde{z}$-domain) with $\gamma = 0.4156$, and the back-transformed identification. Fig. 10(a) shows that warping with $\gamma = 0.4156$ gives the best identification, which reduces the L_2 error by >73% (from 0.0215 to 0.0057) compared to the original case ($\gamma = 0$). The error plot in Fig. 9(b) shows that the $\tilde{z}$-domain identification error in the low-frequency region is reduced compared to the z-domain identification, due to the emphatic macromodeling in the low-frequency region. In this example, the warped identification converged within nine iterations for each γ, and the final solution converged within six iterations (2.29 s) in the bisection method process.

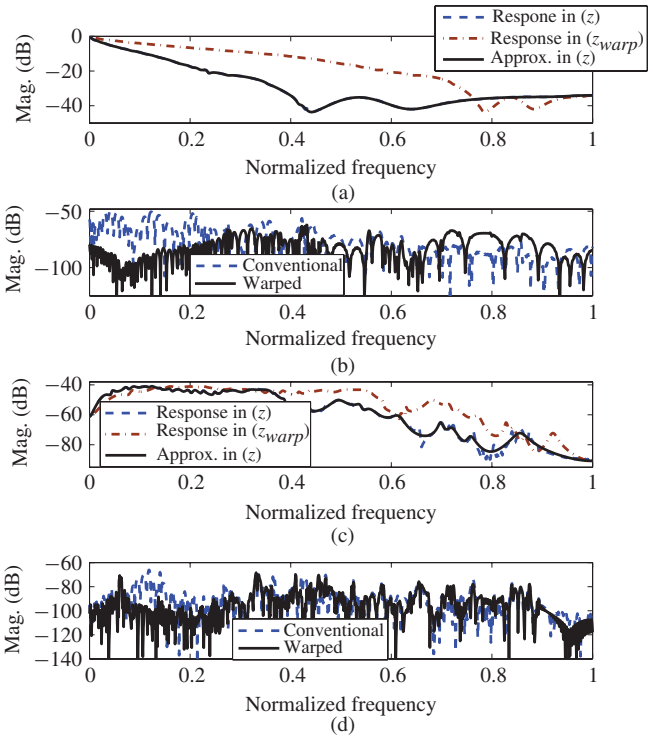

Fig. 9. Responses of the backplane modeling using frequency warping. The differential channel with $\gamma = 0.4156$. (a) Frequency responses. (b) Its identification error. The crosstalk between two channels with $\gamma = 0.4156$. (c) Frequency responses. (d) Its identification error. Here (z) and (z_{warp}) represent the z-domain and $\tilde{z}$-domain, respectively.

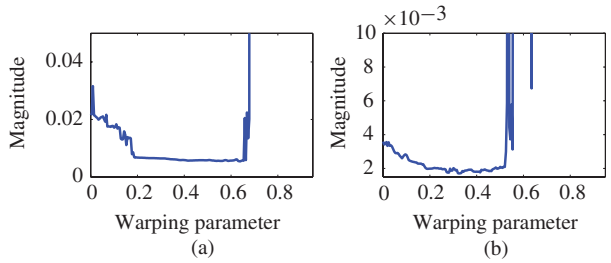

Fig. 10. L_2 error in two macromodeling examples using frequency warping. (a) Channel. (b) Crosstalk.

Furthermore, the maximum condition number of B in (11) decreases significantly (from 1.6×10^{16} to 2.3×10^{4}), as shown in Fig. 11. Therefore, it shows that an appropriate warping can improve the numerical condition and the accuracy of the identification. The crosstalk between two differential channels is also modeled to generate a 60th-order macromodel with the same warping configuration, whose frequency responses and identification errors are shown in Fig. 9(c) and (d), respectively. The L_2 error of crosstalk macromodeling using WISE is reduced by >48% (from 0.0035 to 0.0018).

In the above examples, the warped response is most linearized for the differential channel with $\gamma = 0.5$, which also gives a good fitting. It shows the γ, where $\min_{-1<\gamma<1} \left|(d^2/d\tilde{z}^2)G(\tilde{z})\right|$, can serve as a promising choice of the warping parameter.

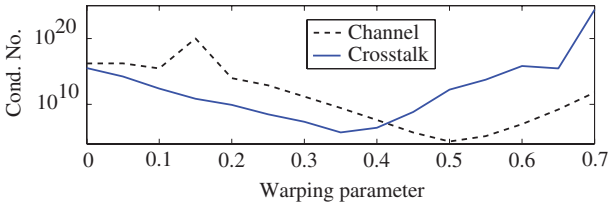

Fig. 11. Maximum condition number during iterative calculations in two macromodeling examples using frequency warping with $0 \le \gamma \le 0.7$.

VI. Conclusion

WISE has been presented for the efficient generation of discrete-time domain macromodels. It has been shown that WISE constitutes a simplified MIMO SM iteration without pole-sensitive computations and initial guess assignment. The macromodel parameters can be efficiently obtained from an allpass operator design process. Model order selection and P-norm identification have been proposed to automate the macromodeling process. Furthermore, frequency warping has been introduced as a pre-processing step to improve the numerical condition. Examples have confirmed that the superiority of WISE over conventional algorithms.

References

[1] B. Gustavsen and A. Semlyen, "Rational approximation of frequency domain responses by vector fitting," *IEEE Trans. Power Delivery*, vol. 14, no. 3, pp. 1052–1061, Jul. 1999.

[2] I. Munteanu and D. Ioan, "Parameter extraction for microwave devices based on 4SID techniques," *IEEE Trans. Magn.*, vol. 35, no. 3, pp. 1781–1784, May 1999.

[3] Y. Hua and T. K. Sarkar, "Generalized pencil-of-function method for extracting poles of an EM system from its transient response," *IEEE Trans. Antennas Propagat.*, vol. 37, no. 2, pp. 229–234, Feb. 1999.

[4] S. Grivet-Talocia, F. G. Canavero, I. S. Stievano, and I. A. Maio, "Circuit extraction via time-domain vector fitting," in *Proc. Int. Symp. Electromagn. Compat.*, vol. 3. Aug. 2004, pp. 1005–1010.

[5] C. U. Lei and N. Wong, "Efficient linear macromodeling via discrete-time time-domain vector fitting," in *Proc. 21st Int. Conf. VLSI Design*, Hyderabad, India, Jan. 2008, pp. 469–474.

[6] C. U. Lei, H. K. Kwan, Y. Liu, and N. Wong, "Efficient linear macromodeling via least-squares response approximation," in *Proc. IEEE Symp. Circuits Syst.*, Seattle, WA, May 2008, pp. 2993–2996.

[7] C. U. Lei and N. Wong, "VISA: Versatile impulse structure approximation for time-domain linear macromodeling," in *Proc. 15th Asia South Pacific Design Autom. Conf.*, Taipei, Taiwan, Jan. 2010, pp. 37–42.

[8] H. Brandenstein and R. Unbehauen, "Least-squares approximation of FIR by IIR digital filters," *IEEE Trans. Signal Process.*, vol. 46, no. 1, pp. 21–30, Jan. 1998.

[9] S. Grivet-Talocia, "Package macromodeling via time-domain vector fitting," *IEEE Microw. Guided Wave Lett.*, vol. 13, no. 11, pp. 472–474, Nov. 2003.

[10] N. Wong and C. U. Lei, "IIR approximation of FIR filters via discrete-time vector fitting," *IEEE Trans. Signal Process.*, vol. 56, no. 3, pp. 1296–1302, Mar. 2008.

[11] L. Naredo, A. Ramirez, A. Ametani, A. Gutierrez, A. Mansoldo, A. Gole, A. Lima, A. Morched, B. Gustavsen, D. Wilcox, F. Uribe, F. Moreira, F. de Leon, J. Martinez, L. Guardado, M. Davila, M. Ritual, N. Nagaoka, N. Watson, P. Gomez, P. Moreno, R. Iravani, S. Carneiro, T. Noda, V. Dinavahi, V. Ortiz, and W. Neves, "z-transform-based methods for electromagnetic transient simulations," *IEEE Trans. Power Delivery*, vol. 22, no. 3, pp. 1799–1805, Jul. 2007.

[12] J. L. Walsh, *Interpolation and Approximation by Rational Functions in the Complex Domain*. Providence, RI: AMS, 1965.

[13] P. A. Regalia, M. Mboup, and M. Ashari, "A class of first- and second-order interpolation problems in model reduction," *AEU Int. J. Electron. Commun.*, vol. 49, pp. 332–343, Sep. 1995.

[14] S. Grivet-Talocia and A. Ubolli, "A comparative study of passivity enforcement schemes for linear lumped macromodels," *IEEE Trans. Adv. Packag.*, vol. 31, no. 4, pp. 673–683, Nov. 2008.
[15] J. O. Smith, *Physical Audio Signal Processing*. W3K Publishing, 2010.
[16] J. O. Smith, *Spectral Audio Signal Processing*. W3K Publishing, 2009.
[17] K. Steiglitz and L. E. McBride, "A technique for the identification of linear systems," *IEEE Trans. Autom. Control*, vol. 10, no. 4, pp. 461–464, Oct. 1965.
[18] M.-H. Cheng and V. Stonick, "Convergence, convergence point and convergence rate for Steiglitz-McBride method; a unified approach," in *Proc. Int. Conf. Acoust., Speech, Signal Process.*, vol. 3. Adelaide, Australia, Apr. 1994, pp. 477–480.
[19] G. Gu, "All optimal Hankel-norm approximations and their $\mathcal{L}_\infty$ error bounds in discrete-time," *Int. J. Control*, vol. 78, no. 6, pp. 408–423, Apr. 2005.
[20] T. Young and W. Huggins, "'Complementary' signals and orthogonalized exponentials," *IRE Trans. Circuit Theory*, vol. 9, no. 4, pp. 362–370, Dec. 1962.
[21] D. Deschrijver and T. Dhaene, "Univariate rational macromodeling of high-speed passive components: A comparative study," *Appl. Comput. Electromagn. Soc. Newslett.*, vol. 20, no. 2, pp. 35–60, Jul. 2005.
[22] G. H. Golub and C. F. V. Loan, *Matrix Computations*, 3rd ed. London, U.K.: Johns Hopkins Univ. Press, 1996.
[23] M. Grant and S. Boyd. *CVX: MATLAB Software for Disciplined Convex Programming* [Online]. Available: http://stanford.edu/∼boyd/cvx/
[24] *Official Website of IdemWorks* [Online]. Available: http://www.idemworks.com/
[25] A. Oppenheim and R. Schaffer, *Discrete-Time Signal Processing*. Englewood Cliffs, NJ: Prentice-Hall, 1999.
[26] T. Parks and C. Burrus, *Digital Filter Design*. New York: Wiley, 1987.
[27] *Official Website of MATLAB RF Toolbox* [Online]. Available: http://www.mathworks.com/products/rftoolbox/
[28] D. Ioan and G. Ciuprina, "Reduced order models of on-chip passive components and interconnects, workbench and test structures," in *Model Order Reduction: Theory, Research Aspects and Applications*. New York: Springer-Verlag, 2008, pp. 447–467.

Chi-Un Lei received the B.E. (with first class honors) and Ph.D. degrees in electrical and electronic engineering from the University of Hong Kong, Pokfulam, Hong Kong, in 2006 and 2011, respectively.

He is currently a Teaching Assistant with the Department of Electrical and Electronic Engineering, University of Hong Kong. His current research interests include very-large-scale integration signal integrity analysis, circuit simulation, and engineering education.

Dr. Lei was awarded with the Best Student Paper Award in IAENG IMECS in 2007 and 2010. He received the Best Poster Award in IEEE ASP-DAC Student Forum in 2010. He is currently a Co-Editor-in-Chief of the International Journal of Design, Analysis and Tools for Integrated Circuits and Systems.

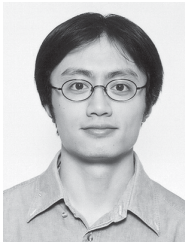

Ngai Wong (S'98–M'02) received the B.E. (with first class honors) and Ph.D. degrees in electrical and electronic engineering from the University of Hong Kong, Pokfulam, Hong Kong, in 1999 and 2003, respectively.

He was an Intern with Motorola, Inc., Hong Kong, from 1997 to 1998, specializing in product testing. He was a Visiting Scholar with Purdue University, West Lafayette, IN, in 2003. He is currently an Associate Professor with the Department of Electrical and Electronic Engineering, University of Hong Kong. His current research interests include very-large-scale integration (VLSI) model order reduction and simulation, digital filter designs, sigma-delta modulators, and optimization problems in communication and VLSI applications.